Neural Correlates of Visual Feature Binding

Tony Ro[1], Allison M. Pierce[1], Michaela Porubanova[2], and Miriam San Lucas[1]

Abstract

■ We perceive visual objects as unified although different brain areas process different features. An attentional mechanism has been proposed to be involved with feature binding, as evidenced by observations of binding errors (i.e., illusory conjunctions) when attention is diverted. However, the neural underpinnings of this feature binding are not well understood. We examined the neural mechanisms of feature binding by recording EEG during an attentionally demanding discrimination task. Unlike prestimulus alpha oscillatory activity and early ERPs (i.e., the N1 and P1 components), the N1pc, reflecting stimulus-evoked spatial attention, was reduced for errors relative to correct responses and illusory conjunctions. However, the later sustained posterior contralateral negativity, reflecting visual short-term memory, was reduced for illusory conjunctions and errors compared with correct responses. Furthermore, binding errors were associated with distinct posterior lateralized activity during a 200- to 300-msec window. These results implicate a temporal binding window that integrates visual features after stimulus-evoked attention but before encoding into visual short-term memory. ■

INTRODUCTION

We typically perceive objects as coherent, unitary percepts, although the individual features (e.g., color, shape, motion) that make up the object are processed in different parts of the brain. For example, when viewing a basketball, we do not perceive the round shape and orange color of the ball separately. Rather, our percept is integrated, and we perceive a round, orange object. The question of how individual features become integrated in the brain is known as the "binding problem" (Treisman, 1996; Treisman & Gelade, 1980).

One of the most influential theories regarding the binding problem is the feature integration theory (FIT; Treisman & Gelade, 1980), which proposes that attention is the mechanism by which individual features are bound together. According to FIT, individual features of an object are processed in separate sensory feature maps, and when attention is focused on the object's location, these features are integrated into a coherent percept (Treisman & Gelade, 1980). This idea is supported by the occurrence of feature-binding errors, or illusory conjunctions (ICs), when attention is diverted (Treisman & Schmidt, 1982). For example, if an observer is presented with a blue triangle and a red diamond but their attention is diverted, the observer may incorrectly report seeing a red triangle rather than a blue triangle because they have incorrectly bound one object's color to the other object's shape. Other studies have shown that the rates of illusory conjunctions are higher in patients with attentional deficits after damage to the parietal lobe (Robertson, 1999; Friedman-Hill, Robertson, & Treisman, 1995; Cohen & Rafal, 1991), further supporting the role of attention in feature binding.

The neural mechanisms of how feature integration occurs are not entirely clear, but one prominent hypothesis proposes that feature binding occurs through reentrant processing (Bouvier & Treisman, 2010; Di Lollo, Enns, & Rensink, 2000; Lamme & Roelfsema, 2000; Treisman & Gelade, 1980). According to this hypothesis, individual features are first processed in early visual areas in a feedforward manner, and conjunctions of features are subsequently determined through a reentrant process in which information is fed back to early visual areas. Support for the reentrant hypothesis comes from behavioral studies that use visual masking to interrupt feedback processing (Bouvier & Treisman, 2010; Di Lollo et al., 2000). This work has shown that interrupting the reentrant process via a visual mask impairs feature binding, resulting in an increase in the number of ICs that occur (Bouvier & Treisman, 2010). Although this behavioral work has suggested that feature binding occurs through reentrant processing (Bouvier & Treisman, 2010), different hypotheses for the neural underpinnings and time course of feature binding have been advanced (Roelfsema, 2023; Vinck et al., 2023; Fries, 2014; Lamme & Roelfsema, 2000; Singer & Gray, 1995).

In the current study, we examined the neural mechanisms of feature binding in humans using EEG. Participants performed an attentionally demanding task optimized to induce a high rate of illusory conjunctions. Our experimental design allowed us to examine neural activity associated with successful feature binding (correct responses), feature-binding errors (illusory conjunctions),

[1]The Graduate Center of the City University of New York, [2]The State University of New York at Farmingdale

and other types of errors. Given the role of attention proposed by FIT (Treisman & Gelade, 1980), we were especially interested in prestimulus oscillatory activity in the alpha frequency range (8–12 Hz), which has been shown to influence subsequent target processing (Ro, 2019; Mathewson et al., 2014; Mathewson, Gratton, Fabiani, Beck, & Ro, 2009; Ergenoglu et al., 2004), as well as poststimulus alpha power changes, which reflect changes in attentional allocation (Foster, Bsales, & Awh, 2020; Hakim, Adam, Gunseli, Awh, & Vogel, 2019; Worden, Foxe, Wang, & Simpson, 2000) and neural feedback processing (van Kerkoerle et al., 2014). We hypothesized larger prestimulus alpha power and opposite prestimulus alpha phase angles for illusory conjunctions compared with correct responses (cf. Mathewson et al., 2009). However, if feedback plays a prominent role in feature binding, and as alpha oscillations have been shown to reflect feedback processing (van Kerkoerle et al., 2014), poststimulus alpha changes may be measured. We also predicted smaller amplitudes for illusory conjunctions compared with correct responses in both the N1pc component, which precedes the later N2pc component (Luck, Girelli, McDermott, & Ford, 1997; Luck & Hillyard, 1994) and reflects initial attentional orienting (Wascher & Beste, 2010), and the sustained posterior contralateral negativity (SPCN) component, an ERP component implicated in visual short-term memory (Prime, Pluchino, Eimer, Dell'Acqua, & Jolicœur, 2011; Robitaille & Jolicoeur, 2006).

METHODS

Participants

Twenty-seven adults with normal or corrected-to-normal vision participated in this experiment. Participants were recruited from either the City University of New York or via online advertisements and were paid for their participation. Eight participants were not included in the final analyses because of technical errors in which either the EEG data ($n = 4$) or the stimulus timing information ($n = 4$) was not properly recorded. Data from another participant was excluded from further analyses for low task performance (< 1% correct responses) and an insufficient number of illusory conjunctions (< 1%). Data from the remaining 18 participants (6 female participants, 18 right-handed, mean age = 29.17 years) are included in all subsequent analyses. This sample size was assessed to be sufficient based on similar sample sizes from previous related work (e.g., Zhang, Zhang, Cai, Luo, & Fang, 2019), as well as an a priori power analysis to estimate a sample size for detecting a medium to large effect size (0.7) with 80% power at an α level of .05 using the *pwr* package in R.

Stimuli and Procedures

Participants were seated at a viewing distance of 57 cm from the center of the monitor. The stimuli consisted of an array containing a triangle and a diamond flanked by upright or inverted Ts (0.5° × 1° of visual angle) briefly presented to the left or right (1.5° and 5.5°) of a central fixation cross (0.8° × 0.8°) on a gray (18.5 cd/m^2) background (Figure 1). The shapes were 1° × 1° of visual angle and were positioned 3° and 4° from fixation. The triangle and the diamond could be red (17.4 cd/m^2, Commission Internationale de l'éclairage [CIE] $x = .624$, $y = .343$), green (32.43 cd/m^2, CIE $x = .284$, $y = .612$), or blue (8.60 cd/m^2, CIE $x = .146$, $y = .067$) but were never the same color as each other for a given trial. The triangle, which was always the target shape, could be either upright or inverted. The diamond was always the nontarget item and was used to induce feature-binding errors. These shapes, which shared some overlapping features, were selected to maximize the number of illusory conjunctions because pilot experiments using more distinctive shapes resulted in much fewer illusory conjunctions and other types of errors.[1]

Each trial began with presentation of the central fixation cross for 1000 msec. Following the fixation cross, the stimulus array was presented for 150 msec to the left or right of fixation. A multicolored pattern mask (23.5° × 7.5° of visual angle), which spanned across both sides of fixation, was then presented for 500 msec and was composed of all shape and color combinations. The mask was followed by the first response screen, on which a question mark was shown at the center of the screen and the words "SAME" and "DIFFERENT" were written in rectangular boxes in the upper left and upper right quadrants. Participants were to indicate via a mouse click whether the flanking Ts were in the same or different orientations and had up to 1500 msec to respond. The second response screen appeared 1500 msec after the appearance of the first response screen and had a question mark at the center of the screen along with each possible target triangle color and orientation in square outlined boxes. Participants were to indicate what the color and orientation of the triangle was via another mouse click (see Figure 1) and had 1500 msec for the second response. The total duration of each trial was 4650 msec. Participants completed six blocks of 128 trials each for 768 trials while we recorded their brain activity via EEG.

Trials were categorized into conditions based on the participant's response to the orientation and color of the triangle. A trial was classified as a correct response if both the orientation and color were correctly identified. An illusory conjunction was considered to have occurred when the correct orientation was identified with the nontarget's (i.e., the diamond's) color. For example, if the trial contained an inverted green triangle and a blue diamond, a correct response would be selecting the inverted green triangle, and an illusory conjunction would be selecting the inverted blue triangle on the response screen. Other response types (i.e., reports of incorrect triangle orientation or of the color that was not presented) were classified as other nonbinding error trials (see Figure 1B).

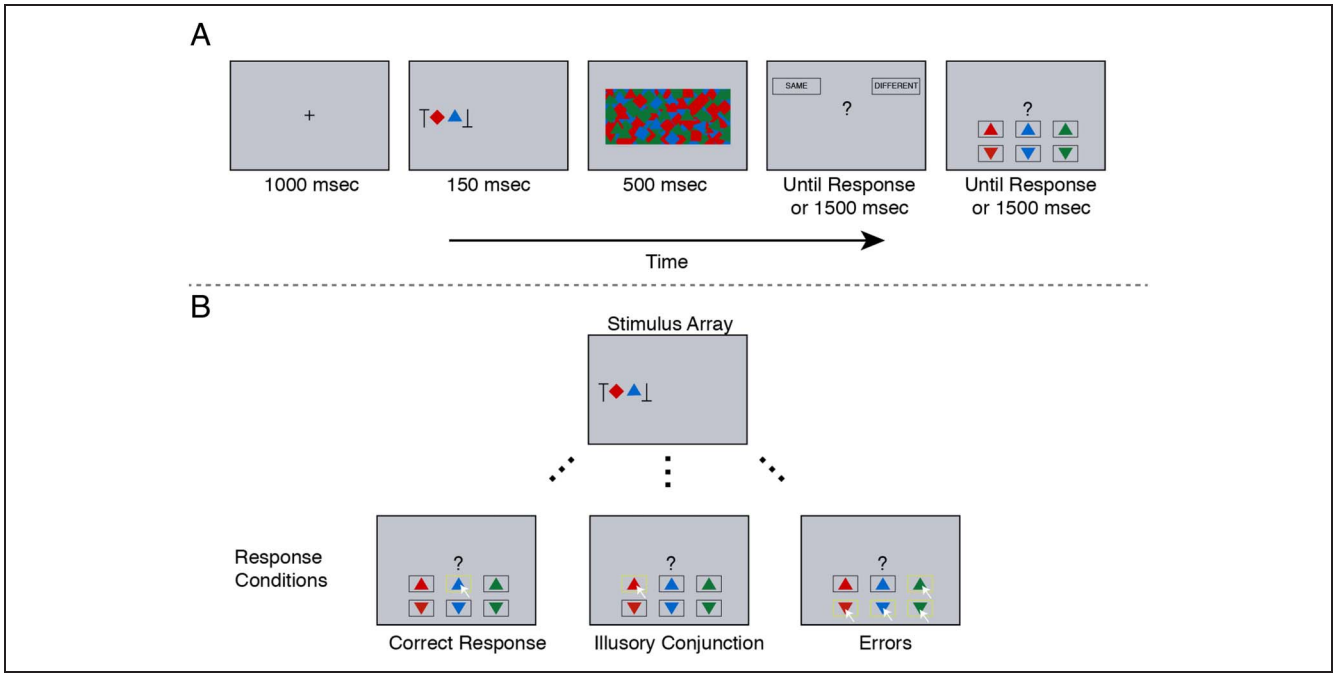

Figure 1. (A) An example of a typical trial sequence in the experiment. Following a fixation point at the center of the screen, the stimuli appeared to the left or right of fixation, followed by a patterned mask. Participants responded first to whether the outer stimuli were the same or different, followed by a response indicating which triangle was presented. (B) Responses were categorized into correct responses (left), illusory conjunctions (middle), and errors (right). White arrows and white boxes, which were not visible to the participants, indicate how these responses would be categorized for this example trial.

EEG Recording and Analysis

Scalp EEG data were recorded from 12 electrodes positioned at F3, Fz, F4, C3 Cz, C4, P3 Pz, P4, O1, Oz, and O2 using Grass amplifiers (Grass Instruments/Natus Medical Inc.). The electrode position coordinates were determined using the International 10–20 electrode placement system. Eye movements and blinks were monitored via EOG recorded from channels positioned above and below the left eye and lateral to the outer canthus of the right eye. Any trials containing oculomotor artifacts (i.e., eye movements or blinks) were rejected via manual inspection and excluded from any further analyses. EEG activity was referenced online to the left mastoid and rereferenced offline to the average of both left and right mastoids. The continuous EEG signal was sampled at a rate of 1000 Hz with an online bandpass filter of 0.1–100 Hz.

We first examined whether oscillatory activity before and at the onset of the target stimulus was involved in feature binding based on claims that synchronized oscillations in the brain may play a critical role in the feature-binding process (Tallon-Baudry & Bertrand, 1999; Singer & Gray, 1995). Because of the low and unreliable power measured in the gamma oscillatory frequency band with scalp electrodes (Yuval-Greenberg, Tomer, Keren, Nelken, & Deouell, 2008), we focused on the activity in the alpha (8–12 Hz) frequency range. We also focused on alpha oscillations because previous work has shown that alpha is related to conscious perception (Ro, 2019; Mathewson et al., 2014; Mathewson et al., 2009; Ergenoglu et al., 2004), attention (Worden et al., 2000), and feedback processing (van Kerkoerle et al., 2014).

For the prestimulus alpha analyses, the continuous EEG data were segmented into 1000-msec epochs beginning 950 msec before the onsets of the stimulus arrays and ending 50 msec after stimulus onset. For the poststimulus alpha analyses, the continuous EEG data were segmented into 1000-msec epochs beginning 200 msec before stimulus onset and ending 800 msec after stimulus onset. Power and phase values in the alpha frequency band (8–12 Hz) were first extracted by convolving each epoch with a set of Morlet wavelets, with frequencies ranging from 8 Hz to 12 Hz in 1-Hz increments. Alpha power and phase estimates were then computed at each participant's peak alpha power frequency, which was defined as the frequency with maximum power after averaging across trials at electrode Pz for the prestimulus analyses and during a time window from −200 msec to stimulus onset at electrodes contralateral to the stimuli for the poststimulus analyses (i.e., averages of electrode P3 for right stimuli and P4 for left stimuli). For both power and phase estimates, trials for each of the response type conditions were then averaged across both sides of stimulus presentation for the prestimulus analyses and separately for contralateral and ipsilateral stimulus presentations for the poststimulus analyses. Alpha power estimates for each response type were then normalized relative to the mean of all trials for the prestimulus analyses and relative to the −200 msec

to stimulus onset baseline window for the poststimulus analyses, yielding measures of relative percent increase or decrease in alpha power.

Next, we were interested in ERPs associated with both early and late processes. We examined the early sensory-related P1 and N1 components, as well as the later N1pc and SPCN components. For these ERP analyses, the continuous EEG data were filtered offline with a Butterworth low-pass filter (30 Hz) and then segmented into 850-msec epochs, beginning 200 msec before the onsets of the stimulus arrays and extending 650 msec poststimulus. The ERPs were baseline-corrected using the 200 msec before stimulus onset. The amplitudes of the P1 and N1 components were measured at the midline occipital electrode (Oz). The P1 and N1 were quantified as the mean amplitude in the 125- to 150-msec and 175- to 200-msec time windows, respectively, following stimulus onset. For examining the N1pc and SPCN components, lateralized contralateral waveforms were computed by averaging the activity recorded from left electrodes when right stimulus arrays were presented with the activity recorded from right electrodes when left stimulus arrays were presented. Separate averaged waveforms were calculated for each of the response types (i.e., correct response, illusory conjunction, errors).

The amplitudes of the N1pc and the SPCN components were measured at occipital electrodes (O1/O2), which were the closest electrodes in our montage to PO7 and PO8, where the N1pc and SPCN are most typically measured. The N1pc was quantified as the mean amplitude in the 150- to 200-msec time window after stimulus onset (cf. Wascher & Beste, 2010). The SPCN component was measured as the mean amplitude in a time window beginning at 300 msec poststimulus (Robitaille & Jolicoeur, 2006) and ending 650 msec poststimulus (i.e., at the offset of the mask). For both the N1pc and SPCN, difference waveforms were calculated by subtracting the ipsilateral from the contralateral waveforms.

Last, in addition to analyzing stimulus-locked ERPs, we also examined response-locked waveforms to see if there were any differences between processing feature-binding errors and the other types of errors. Previous research has shown that the error-related negativity (ERN; Gehring, Goss, Coles, Meyer, & Donchin, 1993) ERP component is elicited when participants commit an error, and some studies have found that this component is reduced when the error is not consciously detected (Wessel, Danielmeier, & Ullsperger, 2011; Maier, Steinhauser, & Hübner, 2008; but see Nieuwenhuis, Ridderinkhof, Blom, Band, & Kok, 2001). Therefore, we also analyzed the ERN component to determine whether there were differences in error processing for feature-binding errors relative to other types of errors.

To examine the ERN, we time-locked the waveforms to the onset of the participant's response and then averaged the waveforms across trials for each response type. Similar to the stimulus-locked waveforms, the response-locked waveforms were baseline corrected using the 200 msec before the onset of the response. Because the ERN is a relative negativity between correct and error responses, we quantified the ERN by subtracting the error waveforms (i.e., illusory conjunctions and errors) from the correct response waveform. We measured the ERN at electrode Cz from the onset of the response until 150 msec postresponse (Wessel et al., 2011; Nieuwenhuis et al., 2001; Gehring et al., 1993).

RESULTS

Behavioral Results

Trials were categorized into different response types as shown in Figure 1B. Although there were six response options, we combined responses that were not correct responses or illusory conjunctions into a single category of general errors. The four collapsed error types were unable to be analyzed separately because of low trial numbers in several of the error types. Thus, the three response types analyzed were correct responses, illusory conjunctions, and errors.

A one-way repeated-measures ANOVA indicated that there were differences in the rates of occurrence among these three response types, $F(2, 34) = 17.23$, $p < .001$, $\eta_p^2 = .50$. Participants had more correct responses ($M = 35.29\%$, $SD = 9.24$) than illusory conjunctions ($M = 23.17\%$, $SD = 4.53\%$, $p = .001$, false discovery rate (FDR) corrected, Cohen's $d = 1.04$). Errors ($M = 41.54\%$, $SD = 8.74\%$) occurred more frequently than illusory conjunctions ($p < .001$, FDR corrected, Cohen's $d = 1.76$), but did not statistically differ from the proportion of correct responses ($p = .146$, FDR corrected). Although the intentional difficulty of the task resulted in a relatively low proportion of correct responses (35.29%), this level of performance was still significantly above chance levels (16.67%), $p < .001$, $\varphi = 0.50$, indicating participants were performing appropriately given the task difficulty. Importantly, the task elicited an adequate number of illusory conjunctions (23.17%) for our electrophysiological data analyses.

To assess whether trials categorized as illusory conjunctions were "true" illusory conjunctions or the result of guessing, we used multinomial modeling to assess guessing rates (Esterman, Prinzmetal, & Robertson, 2004; Prinzmetal, Ivry, Beck, & Shimizu, 2002; Ashby, Prinzmetal, Ivry, & Maddox, 1996). This approach accounts for all the possible ways in which a particular outcome (e.g., correct feature binding, illusory conjunction) may occur. For example, a response categorized as an illusory conjunction may occur because the observer conjoined the color of the nontarget item with the shape of the target item, perceiving the target item as the nontarget item's color, or this same response may occur because the observer failed to perceive the color of the target item entirely and guessed the nontarget's color. This multinomial

Table 1. Response Proportions (Actual and Predicted) by Response Type

	Response Proportion	
Response Type	*Actual Value*	*Predicted Value*
Correct response	0.36	0.34
Illusory conjunction	0.23	0.25
Other color error + correct orientation	0.03	0.03
Color correct + orientation error	0.19	0.21
Illusory color + orientation error	0.17	0.15
Other color error + orientation error	0.02	0.02

modeling approach better estimates the true probabilities of each outcome using a model based on the psychological parameters that could lead to a given outcome (Prinzmetal et al., 2002). We used the same following parameters in our model as in similar studies (Esterman et al., 2004; Prinzmetal, Henderson, & Ivry, 1995). These include the probability of correctly identifying the target's orientation, *P*(target orientation), the target's color, *P*(target color), the nontarget's color, *P*(nontarget color), and the probability of correctly conjoining the target's color and orientation, denoted by α (Table 1). The α parameter, representing the probability of correctly binding the target's features, is the critical parameter for examining illusory conjunctions, with a value of 1.0 reflecting perfect feature binding and a value of 0.5 reflecting chance binding (Esterman et al., 2004; Prinzmetal et al., 2002; Prinzmetal et al., 1995).

We used multiTree (Moshagen, 2010) to create a probability tree of all possible ways in which our parameters might lead to a particular response outcome (e.g., see Esterman et al., 2004; Prinzmetal et al., 2002, 1995), and subsequently fit the model for each participant. Table 1 shows the empirically measured proportions and model-predicted proportions, and Table 2 shows the parameter estimates averaged across participants.[2] Our α parameter estimate (.58) is similar to those observed in a previous study with a similar paradigm (.62 and .65; Esterman et al., 2004), indicating that many of the conjunction responses we measured likely reflected true illusory conjunctions rather than random guessing.

Table 2. Model Parameters

Model Parameter	*Estimated Value*
P (target orientation)	0.24
P (target color)	0.90
P (nontarget color)	0.88
P (α)	0.58

Parameters indicate the probability of correctly perceiving the target's orientation, the target's color, the nontarget's color, and the probability of correctly conjoining the target orientation with the target color (α).

We also compared the α parameter estimates of participants with high compared with low rates of illusory conjunctions, which was determined by a median split. Participants with high rates of illusory conjunctions had significantly lower α parameter estimates ($M = .52$, $SD = .03$) than those with low rates of illusory conjunctions (α parameter estimate: $M = .62$, $SD = .08$), $t(15) = 3.34$, $p = .005$, Cohen's $d = 1.62$. This is in line with our multinomial modeling approach in which a higher α estimate indicates a higher probability of correctly binding the two target features (thus, a lower probability of illusory conjunctions).

EEG Results

A median of 9.51% of the trials were rejected because of oculomotor artifacts (i.e., blinks or eye movements), which were determined by consensus of two of the coauthors (M.P. and M.S.L.) after independent visual inspections of the EEG data. The remaining trials without blinks or eye movements were used for the remainder of the analyses.

Prestimulus Oscillatory Activity

Because oscillatory activity in the alpha (8–12 Hz) frequency range has previously been associated with attention (Worden et al., 2000) and conscious perception (Ro, 2019; Mathewson et al., 2009; Ergenoglu et al., 2004), we first examined whether alpha activity before and at stimulus onset played a role in feature binding. One-way ANOVAs were used to compare prestimulus alpha power as well as the alpha power and phase at stimulus onset at electrode Pz for the different response types. Alpha power estimates for each response type were normalized relative to the mean of all trials, yielding a measure of relative percent increase or decrease in power.

Although Figure 2A shows that there was a small relative increase in alpha power at stimulus onset for illusory conjunctions ($M = 0.51$, $SD = 15.03$) and small relative decreases in power for correct responses ($M = -0.15$, $SD = 7.02$) and errors ($M = -0.77$, $SD = 6.92$), there were no statistical differences in alpha power among the three

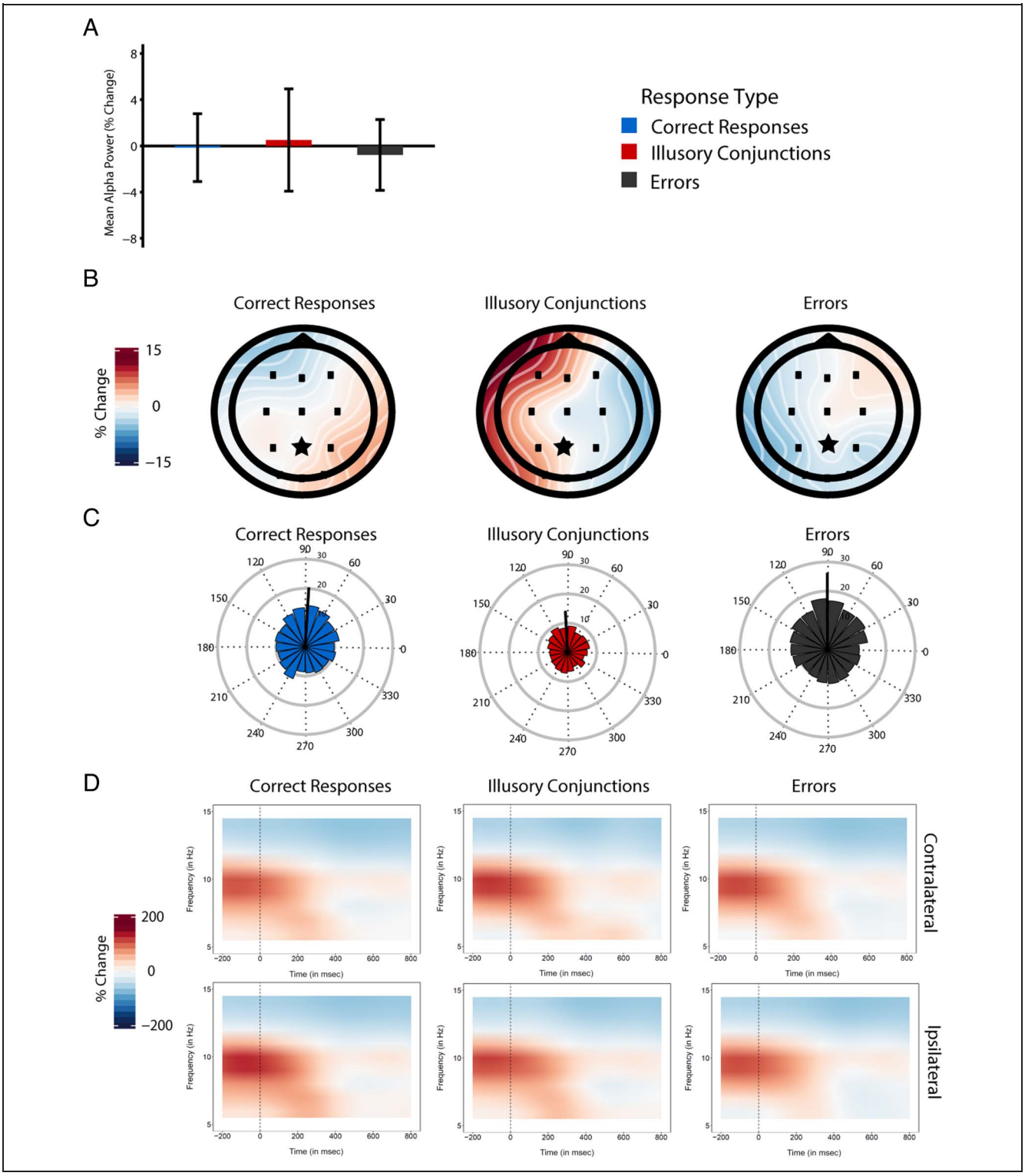

Figure 2. (A) Bar graph of alpha amplitudes at electrode Pz and (B) scalp maps show normalized alpha power at stimulus onset. (C) Alpha phase data at stimulus onset at electrode Pz. Plots show phase cycle divided into 18 bins (20° each) with the vectors representing how many trials on average were in each bin. The black line in each plot represents the mean direction and vector length across all participants for each response type. (D) Normalized contralateral and ipsilateral alpha band power changes from 200 msec before stimulus onset through 800 msec after stimulus onset averaged across electrodes P3 and P4.

response types, $F(2, 34) = 0.05$, $p = .952$. We also examined alpha power before stimulus onset by averaging power estimates across the entire prestimulus epoch. However, prestimulus alpha also did not differ among correct responses ($M = 1.38$, $SD = 6.42$), illusory conjunctions ($M = -0.74$, $SD = 11.52$), and errors ($M = -1.23$, $SD = 4.81$), $F(2, 34) = 0.37$, $p = .693$. Bayesian analyses confirmed support for the null hypothesis that there

Table 3. Posterior Estimates and 95% HPD Intervals for Alpha Phase for Each Response Type

Response Type	*Mean*	*SD*	*Lower HPD*	*Upper HPD*
Correct Response	86.43°	13.31°	59.73°	112.63°
Illusory Conjunction	93.47°	14.91°	62.01°	121.12°
Error Response	93.70°	7.77°	78.68°	109.23°

were no differences in alpha power before and at stimulus onset between the different conditions, Bayes Factor (BF_{10}) = 0.214 and BF_{10} = 0.152, respectively.

For the phase of alpha at stimulus onset, Rayleigh's tests confirmed that the distribution of phase angles for all three response types were not uniform, indicating that there was a concentration of phases toward a specific angle for correct responses, $p = .002$, illusory conjunctions $p = .004$, and errors, $p < .001$. We then used Kuiper's tests to directly compare the distributions for each response type to each other. However, contrary to our prediction, none of the distributions of phase angles among the three response types varied significantly from each other, all ps > .529 (Figure 2C).

We also employed a Bayesian analysis for the phase angles. Because phase angles are circular, rather than linear, we performed this analysis by using the *bpnreg* (Cremers, 2018) package in R, which uses a Bayesian method to fit a circular mixed effects model (for examples and a detailed explanation of this analysis, see Cremers & Klugkist, 2018). As can be seen in Table 3 and in line with the results from the Kuiper's tests mentioned above, the 95% highest posterior density intervals for the parameter estimates of each response type overlap, indicating that the circular means for alpha phase at onset did not differ by response type.

Poststimulus Alpha Activity

Because alpha oscillations have also been suggested to reflect feedback processing (van Kerkoerle et al., 2014) and poststimulus allocation of attention (Foster et al., 2020; Hakim et al., 2019; Worden et al., 2000), we next examined whether there were any differences between the response types in a poststimulus alpha power window from stimulus onset to 800 msec after stimulus onset. Figure 2D shows similar levels of alpha power suppression after stimulus onset, regardless of the side of the stimuli or the response type. A two-way ANOVA with laterality (contralateral, ipsilateral) and response type (correct, ICs, errors) as the two within-subject factors showed no significant main effects of Laterality, $F(1, 17) = 2.848$, $p = .110$, or Response Type, $F(2, 34) = 0.500$, $p = .611$, and no Laterality × Response Type interaction, $F(2, 34) = 1.543$, $p = .228$. We also analyzed whether there were any poststimulus alpha power differences in each of five different ERP time windows (P1, N1, N1pc, a 200- to 300-msec binding window, and SPCN) using five separate two-way ANOVAs with Laterality (contralateral, ipsilateral) and Response Type (correct, ICs, errors) as the two within-subject factors. These analyses showed only a significant main effect of Laterality, with greater contralateral than ipsilateral alpha suppression, during the SPCN time window, $F(1, 17) = 4.832$, $p = .0421$. This main effect of Laterality during the 300- to 650-msec SPCN time window likely reflects a differential allocation of attention contralateral to the stimuli and is consistent with Hakim and colleagues (2019), who showed distinct types of lateralized alpha changes beginning around 300 msec in different attention and working memory tasks but for a longer 400- to 1450-msec analysis time window. Bayesian analyses confirmed support for the null hypothesis that there were no differences in lateralized (i.e., contralateral minus ipsilateral) alpha power changes between the different response type conditions across or for any of the poststimulus time windows, all BF_{10}s < 0.686.

Stimulus-locked ERPs

To examine processes associated with early target processing, we analyzed the early visual ERP components. As shown in Table 4, there were no differences among the different response types for the P1 component, $F(2, 34) = 0.17$, $p = .847$, $BF_{10} = 0.161$. Similarly, the N1 component also did not vary among correct responses, illusory conjunctions, and errors, $F(2, 34) = 1.45$, $p = .248$, $BF_{10} = 0.394$.

Table 4. Mean Amplitude and Standard Deviations for P1, N1, P2, N2, and P3 visual Components From Electrode Oz

	P1	*N1*	*P2*	*N2*	*P3*
Response Type	*M (SD)*	*M (SD)*	*M (SD)*	*M (SD)*	*M (SD)*
Correct	1.67 (0.31)	0.70 (0.18)	1.21 (0.25)	−5.43 (0.72)	5.90 (1.51)
Illusory Conjunction	1.53 (0.34)	0.27 (0.21)	0.65 (0.28)	−6.30 (0.76)	5.36 (1.47)
Error Trials	1.64 (0.38)	0.42 (0.15)	0.91 (0.26)	−5.69 (0.69)	5.66 (1.47)

Together, these results suggest that feature binding processes are not reflected at these early sensory encoding stages. We also examined the P2 (200–225 msec), N2 (250–300 msec), and the P3 (325–425 msec) components following the P1/N1 components. However, no differences were observed among response types for the P2 component, $F(2, 34) = 2.02$, $p = .148$, $BF_{10} = 0.583$. Similarly, although the ANOVA for the N2 approached significance, $F(2, 34) = 2.83$, $p = .073$, $\eta_p^2 = .14$, $BF_{10} = 0.999$, none of the post hoc comparisons among response types were significant after FDR correction, all ps $> .213$, all $BF_{10} < 1.104$. Last, there were also no differences in the P3 component among response types, $F(2, 34) = 1.12$, $p = .338$, $BF_{10} = 0.318$.

To investigate the later stages of target processing among the different response types, we first analyzed the N1pc component, an index of spatial attention (Wascher & Beste, 2010). As shown in Figure 3, the N1pc component was elicited with larger posterior scalp topography differences in all three conditions and was confirmed by t tests, showing the contralateral waveforms were more negative than the ipsilateral waveforms, all ps $< .001$, FDR corrected, all Cohen's ds > 0.95. A repeated-measures one-way ANOVA computed on the difference waves revealed the N1pc varied among the different trial types, $F(2, 34) = 4.84$, $p = .014$, $\eta_p^2 = .22$. Follow-up pairwise comparisons (FDR corrected) revealed that the N1pc during error trials ($M = -1.98$, $SD = 2.08$) was smaller than for both correct responses ($M = -2.26$, $SD = 2.22$), $p = .041$, Cohen's $d = 0.65$, and illusory conjunctions ($M = -2.26$, $SD = 2.18$), $p = .048$, Cohen's $d = 0.55$. Interestingly, the N1pc did not differ between illusory conjunctions and correct responses, $p = .872$, $BF_{10} = 0.246$, suggesting that the visual features were not yet bound at this stage or that the N1pc is insensitive to the binding process.

To determine whether later visual short-term memory (VSTM) processes are involved in feature binding, we examined the SPCN component. Similar to the N1pc, the SPCN was also observed in all three conditions, shown by the greater negativity for the contralateral compared with ipsilateral waveform in the 300- to 650-msec time window, all ps $< .024$ FDR corrected, all Cohen's ds > 0.58. A repeated-measures one-way ANOVA computed on the difference wave during this time window showed that the SPCN also varied among the different trial types, $F(2, 34) = 4.39$, $p = .020$, $\eta_p^2 = .21$. As shown in Figure 3 and confirmed by FDR-corrected pairwise comparisons, the SPCN elicited during correct responses ($M = -0.92$, $SD = 0.62$) trials was larger than that during both illusory conjunctions ($M = -0.50$, $SD = 0.84$), Cohen's $d = 0.68$, and error trials ($M = -0.54$, $SD = 0.72$), Cohen's $d = 0.61$, both ps $< .030$. However, the SPCN in the illusory conjunction trials was not different than that in the error trials, $p = .842$, $BF_{10} = 0.248$.

These differences between the conditions for the N1pc and the SPCN components were further corroborated by a Condition (Correct, IC, Error) × ERP Component (N1pc/SPCN) ANOVA, which showed a significant main effect of Condition, $F(2, 34) = 4.983$, $p = .013$, $\eta_p^2 = .033$; a significant main effect of ERP Component, $F(1, 17) = 9.744$, $p = .006$, $\eta_p^2 = .955$; as well as a significant Condition × Component interaction, $F(2, 34) = 3.651$, $p = .0366$, $\eta_p^2 = .013$. Together, these N1pc and SPCN results suggest that the binding process is occurring after the N1pc but before the SPCN time windows because the waveforms elicited by correct responses and illusory conjunctions did not differ during the N1pc time window but did differ during the SPCN time window. Thus, we examined the contralateral-minus-ipsilateral scalp topographies across time, beginning at the N1pc window and extending through the SPCN time window. Visual inspection of Figure 3B and C demonstrates that following the posterior negativity of the N1pc, a posterior positivity is briefly observed before the sustained posterior negativity of the SPCN appears. This may reflect the Pd component (Sawaki, Geng, & Luck, 2012; Hickey, Di Lollo, & McDonald, 2009) and might alternatively suggest that attention was prematurely terminated or suppressed before accurate feature binding occurred. In either case, these results further suggest that visual feature binding is occurring between the N1pc and SPCN time windows.

We examined this posterior lateralized activity occurring during the 200- to 300-msec binding window for correct responses and illusory conjunctions by comparing the contralateral to ipsilateral waveforms at electrodes O1/O2. For correct responses, the contralateral waveform was slightly more positive than the ipsilateral waveform, but this difference did not reach statistical significance, $t(17) = 1.71$, $p = .106$, Cohen's $d = 0.40$. The posterior lateralization was more pronounced for illusory conjunctions, as the contralateral waveforms were significantly more positive than the ipsilateral waveforms for this response type, $t(17) = 3.33$, $p = .004$, Cohen's $d = 0.78$. This more pronounced lateralization for illusory conjunctions during the binding window may be indicative of activity that reflects additional processes when feature binding is more difficult or more computations are required, perhaps because attention has been diverted.

Response-locked ERPs

Finally, to determine whether there were differences in error processing for the different conditions (i.e., illusory conjunctions and errors), we also examined the response-locked ERN component (Gehring et al., 1993), baseline corrected to the average voltage of the 200-msec time window before the response. The ERN for each condition was quantified as the difference between incorrect and correct responses during a time window between response onset and 150 msec postresponse. As shown in Figure 4, errors did elicit a small negative deflection ($M = -0.14$, $SD = 0.76$), whereas illusory conjunctions did not ($M = 0.22$, $SD = 1.12$). However, this negativity observed for errors

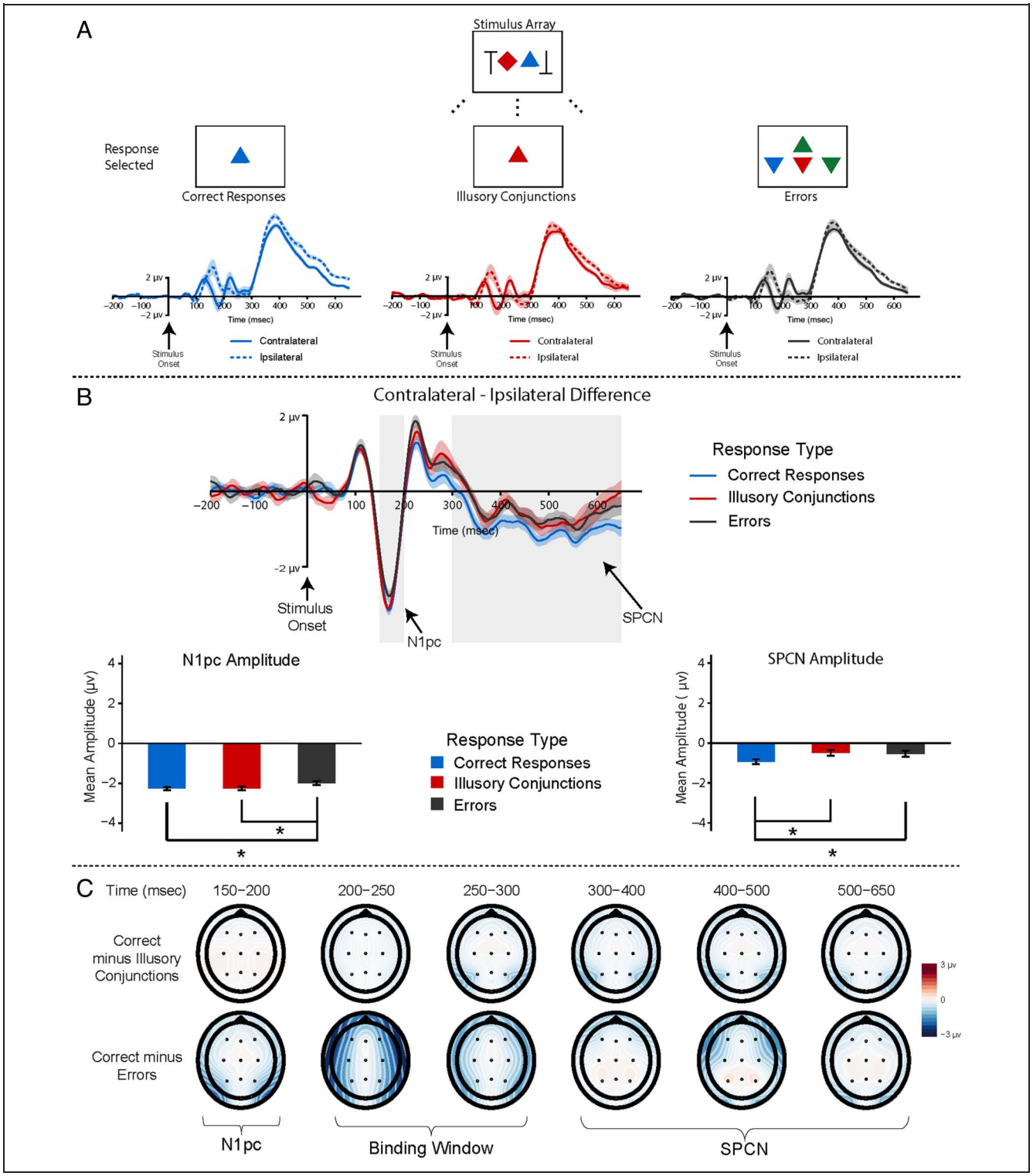

Figure 3. (A) ERP waveforms contralateral (solid lines) and ipsilateral (dashed lines) to the stimulus array for each type of response at posterior electrodes (O1/O2; shaded areas reflect ± 1 *SEM*). (B) Contralateral – ipsilateral difference waveforms and bar graphs for each response type at O1/O2. The gray boxes indicate the time windows analyzed for the N1pc (150–200 msec) and the SPCN (300–650 msec). Bar graphs showing mean amplitudes for N1pc and SPCN components with error bars reflecting ± 1 *SEM*. *Indicates $p < .05$. (C) Scalp topographies (differences) for conditions of interest (correct responses minus illusory conjunctions and correct responses minus errors) throughout N1pc to SPCN time windows.

was not statistically significant, $t(17) = -0.76$, $p = .457$, indicating neither condition elicited a significant ERN component. Interestingly, in an exploratory analysis, we found that when participants indicated that they did not know or were unsure of the identity of the target (i.e., by clicking on the "?" in the center of the response screen), a marginally significant ERN was observed, $t(17) = -1.98$, $p = .065$, Cohen's $d = 0.47$, as shown in Figure 4. Given

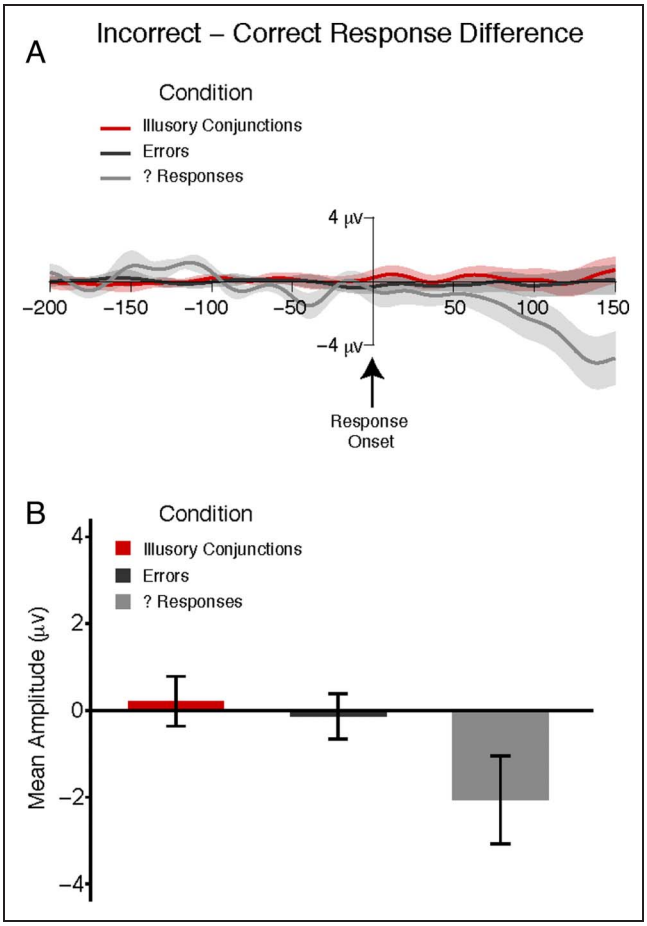

Figure 4. (A) Response-locked difference waves (incorrect – correct response) for illusory conjunctions, errors, and question mark responses at electrode Cz during the 0- to 150-msec time window analyzed (shaded areas reflect ± 1 *SEM*). (B) Mean amplitude of ERN for each response with error bars reflecting ± 1 *SEM*.

this latter result was exploratory and only marginally significant and because the ERN component likely overlapped with the stimulus-evoked P300 on many trials, whether the ERN might reflect errors or failures in binding in this experimental design remains to be determined.

DISCUSSION

The present study examined the neural mechanisms and temporal dynamics of visual feature binding. We found no differences in alpha oscillatory activity between correct binding responses, illusory conjunctions, and errors before, at, or after stimulus onset. There were also no differences in early ERP components associated with sensory processing (i.e., P1 and N1). However, later lateralized neural responses (i.e., N1pc and SPCN) showed differential activity for correct responses, illusory conjunctions, and error trials. More specifically, we found that although the N1pc was larger for correct responses and illusory conjunctions relative to error trials, it did not differ between the former two response types. In contrast, a dissociation between correct responses and illusory conjunctions was observed later during the time window of the SPCN component. Specifically, we found that the SPCN for correct responses was larger than for both error trials and illusory conjunctions.

Although differences in prestimulus and poststimulus alpha do not appear to reflect successful or failed feature binding, arguing against synchrony (Singer & Gray, 1995), coherence (Fries, 2014), and feedback (van Kerkoerle et al., 2014; Bouvier & Treisman, 2010) in feature binding, later processing stages do appear to be involved, providing some support for increases or amplification in neural activity during feature binding (Roelfsema, 2023; Vinck et al., 2023). Our ERP results suggest that feature binding occurred in the temporal window after the N1pc but before the SPCN component. Although we observed a reduced N1pc for error trials relative to illusory conjunction and correct response trials, indicating the stimulus display was not appropriately attended and processed during trials that led to error responses, this was not the case for illusory conjunctions. Rather, a similar neural response was elicited during the N1pc time window for illusory conjunctions and correct responses, suggesting that features are not yet properly bound at this stage because the stimulus displays of both response types appear to be processed in a similar fashion during this time. However, during the later time window of the SPCN, differences in amplitude between correct responses compared with both illusory conjunctions and errors were observed, suggesting feature binding was complete by this stage. It is possible that the larger SPCN we observed for correct responses may reflect the stable, appropriately integrated percept of the target in VSTM. However, it is also possible that the differences in the SPCN component were because of differential allocation of attention (Berggren & Eimer, 2016), as larger illusory conjunction rates have been associated with deficits in attention (Robertson, 1999; Friedman-Hill et al., 1995; Cohen & Rafal, 1991).

In either case, our results indicate that feature binding, or failures thereof, occur during a binding window 200–300 msec poststimulus onset (i.e., following the N1pc but before the SPCN). The outcome of processing during this feature binding window likely resulted in the differences we observed in the SPCN component. Inspection of Figure 3C shows that the scalp topography differences change during the binding window between the N1pc and SPCN components. Notably, this change is observed as lateralized posterior differences, like the lateralized posterior changes observed for the N1pc and SPCN components. Given the lateralized nature of the stimuli in our paradigm and of the visual system, it is not unusual that the activity during this binding window is lateralized, although this may not be the case in other paradigms in which the stimuli and/or the allocation of attention are central. Consistent with the idea that feature binding relies on reentrant processing (Bouvier & Treisman, 2010), the late occurrence and posterior location of activity in the binding window suggests that this activity may reflect

feedback processes that are not necessarily reflected in alpha oscillations. This conclusion is also consistent with previous research that used TMS to interrupt the reentrant process and found that later time windows (from 150 to 240 msec poststimulus onset) of V1/V2 activity are critical for feature binding (Koivisto & Silvanto, 2012).

Although our results provide insight into the neural basis of feature binding, there are a few limitations that the present study cannot address. Previous behavioral work examining the involvement of reentrant processing in feature binding made use of masking to interrupt the reentrant process (Bouvier & Treisman, 2010). Although our paradigm utilized a backward pattern mask to induce illusory conjunctions, we did not include a no mask condition, which limits our conclusions about whether our mask interrupted the reentrant process and directly caused illusory conjunctions to occur. Although the timing of the feature-binding window we observed and the onset of the mask as well as the scalp topography of this binding window are consistent with an explanation of the mask interrupting reentrant processes, future work is necessary to directly test this possibility. A second limitation in our design was the use of fixed temporal intervals for each trial, which may have reduced the ability to detect differences in the power and phase of alpha oscillations. Using temporally jittered intertrial intervals in future studies may reveal alpha oscillation differences between accurate feature binding and illusory conjunctions. Another limitation is related to our findings with the SPCN. Differences in this SPCN component, referred to as the contralateral delay activity in working memory paradigms, have been shown to scale with the number of items held in working memory (Vogel & Machizawa, 2004), but our paradigm did not manipulate the number of target items or the number of features to be integrated. Previous research has also shown that contralateral delay activity amplitude generally depends on number of items rather than number of features stored in VSTM (Luria & Vogel, 2011); however, these previous studies only examined trials with correct responses. Because our goal was to examine the temporal dynamics of feature binding and not the neural dynamics of VSTM capacity, future research is necessary to better understand whether the SPCN reflects failures of encoding conjoined information into VSTM when an illusory conjunction occurs. Finally, the use of a unilateral unbalanced display, in contrast to a bilateral balanced display, precluded the ability to adequately measure an N2pc component. Future studies using bilateral displays may shed further insight into how later attentionally related ERP components may contribute to feature binding.

In conclusion, the present study demonstrates that feature binding primarily occurs between later stages of processing that reflect stimulus-evoked spatial attention (i.e., the N1pc) and visual short-term memory (i.e., the SPCN) processes. This is consistent with the notion that perception results from multiple recurrent feedforward and feedback processing cycles (Enns, 2004; Di Lollo, Enns, & Rensink, 2000) Although both correct responses and illusory conjunctions were initially attended, features were not yet bound at this stage. Rather, our results indicate that the binding process occurred after the N1pc, during a binding window 200–300 msec poststimulus. The outcome of processing during this binding window likely then resulted in the differences observed later in the SPCN. Given the timing of the binding window, our findings support a framework of feature binding in which binding occurs at later feedback stages of processing.

Acknowledgments

We thank Bill Prinzmetal for helpful discussions on this research and for suggesting the multinomial analyses.

Corresponding author: Tony Ro, Programs in Cognitive Neuroscience, Psychology, and Biology, The Graduate Center of the City University of New York, New York, NY 10016, or via e-mail: tro@gc.cuny.edu.

Data Availability Statement

The data are not publicly available because of lack of consent for data sharing from the participants.

Author Contributions

Tony Ro: Conceptualization; Data curation; Formal analysis; Funding acquisition; Methodology; Project administration; Software; Supervision; Visualization; Writing—Original draft; Writing—Review & editing. Allison M. Pierce: Data curation; Formal analysis; Software; Visualization; Writing—Original draft; Writing—Review & editing. Michaela Porubanova: Investigation; Writing—Review & editing. Miriam San Lucas: Investigation; Writing—Review & editing.

Funding Information

This research was supported by the U.S. National Science Foundation (https://dx.doi.org/10.13039/100000001), grant number: BCS #1755477 to T. R.

Diversity in Citation Practices

Retrospective analysis of the citations in every article published in this journal from 2010 to 2021 reveals a persistent pattern of gender imbalance: Although the proportions of authorship teams (categorized by estimated gender identification of first author/last author) publishing in the *Journal of Cognitive Neuroscience* (*JoCN*) during this period were M(an)/M = .407, W(oman)/M = .32, M/W = .115, and W/W = .159, the comparable proportions for the articles that these authorship teams cited were M/M = .549, W/M = .257, M/W = .109, and W/W = .085 (Postle and Fulvio, *JoCN*, 34:1, pp. 1–3). Consequently, *JoCN* encourages all authors to consider gender balance explicitly when

selecting which articles to cite and gives them the opportunity to report their article's gender citation balance.

Notes

1. The use of overlapping features between the triangles and diamonds should not introduce any confounds or other issues in our experimental design, results, or interpretations because the classification of trials into the different response types depended upon whether the orientation of the triangle was correctly perceived with the correct color (correct trials) or with the color of the diamond (illusory conjunction trials). However, this design limits the ability to assess whether an illusory conjunction is the result of incorrect color perception of the triangle or incorrect shape perception of the diamond as a triangle. Future experiments using shapes with nonoverlapping features and with responses that also include the perceived location of the target stimulus may be able to distinguish between these different types of illusory conjunctions.
2. For one participant's data, the algorithm did not converge, and thus accurate parameter estimates could not be obtained. This participants' data were therefore excluded from the multinomial model analysis as well as the median split analysis comparing the α parameter estimates.

REFERENCES

Ashby, F. G., Prinzmetal, W., Ivry, R., & Maddox, W. T. (1996). A formal theory of feature binding in object perception. *Psychological Review*, *103*, 165–192. https://doi.org/10.1037/0033-295x.103.1.165, PubMed: 8650297

Berggren, N., & Eimer, M. (2016). Does contralateral delay activity reflect working memory storage or the current focus of spatial attention within visual working memory? *Journal of Cognitive Neuroscience*, *28*, 2003–2020. https://doi.org/10.1162/jocn_a_01019, PubMed: 27458749

Bouvier, S., & Treisman, A. (2010). Visual feature binding requires reentry. *Psychological Science*, *21*, 200–204. https://doi.org/10.1177/0956797609357858, PubMed: 20424045

Cohen, A., & Rafal, R. D. (1991). Attention and feature integration: Illusory conjunctions in a patient with a parietal lobe lesion. *Psychological Science*, *2*, 106–110. https://doi.org/10.1111/j.1467-9280.1991.tb00109.x

Cremers, J. (2018). Bpnreg: Bayesian projected normal regression models for circular data. https://doi.org/10.32614/CRAN.package.bpnreg

Cremers, J., & Klugkist, I. (2018). One direction? A tutorial for circular data analysis using R with examples in cognitive psychology. *Frontiers in Psychology*, *9*, 2040. https://doi.org/10.3389/fpsyg.2018.02040, PubMed: 30425670

Di Lollo, V., Enns, J. T., & Rensink, R. A. (2000). Competition for consciousness among visual events: The psychophysics of reentrant visual processes. *Journal of Experimental Psychology: General*, *129*, 481–507. https://doi.org/10.1037/0096-3445.129.4.481, PubMed: 11142864

Enns, J. T. (2004). Object substitution and its relation to other forms of visual masking. *Vision Research*, *44*, 1321–1331. https://doi.org/10.1016/j.visres.2003.10.024, PubMed: 15066393

Ergenoglu, T., Demiralp, T., Bayraktaroglu, Z., Ergen, M., Beydagi, H., & Uresin, Y. (2004). Alpha rhythm of the EEG modulates visual detection performance in humans. *Cognitive Brain Research*, *20*, 376–383. https://doi.org/10.1016/j.cogbrainres.2004.03.009, PubMed: 15268915

Esterman, M., Prinzmetal, W., & Robertson, L. (2004). Categorization influences illusory conjunctions. *Psychonomic Bulletin & Review*, *11*, 681–686. https://doi.org/10.3758/BF03196620, PubMed: 15581118

Foster, J. J., Bsales, E. M., & Awh, E. (2020). Covert spatial attention speeds target individuation. *Journal of Neuroscience*, *40*, 2717–2726. https://doi.org/10.1523/JNEUROSCI.2962-19.2020, PubMed: 32054678

Friedman-Hill, S. R., Robertson, L. C., & Treisman, A. (1995). Parietal contributions to visual feature binding: Evidence from a patient with bilateral lesions. *Science*, *269*, 853–855. https://doi.org/10.1126/science.7638604, PubMed: 7638604

Fries, P. (2014). Rhythms for cognition: Communication through coherence. *Neuron*, *88*, 220–235. https://doi.org/10.1016/j.neuron.2015.09.034, PubMed: 26447583

Gehring, W. J., Goss, B., Coles, M. G. H., Meyer, D. E., & Donchin, E. (1993). A neural system for error detection and compensation. *Psychological Science*, *4*, 385–390. https://doi.org/10.1111/j.1467-9280.1993.tb00586.x

Hakim, N., Adam, K. C. S., Gunseli, E., Awh, E., & Vogel, E. K. (2019). Dissecting the neural focus of attention reveals distinct processes for spatial attention and object-based storage in visual working memory. *Psychological Science*, *30*, 526–540. https://doi.org/10.1177/0956797619830384, PubMed: 30817220

Hickey, C., Di Lollo, V., & McDonald, J. J. (2009). Electrophysiological indices of target and distractor processing in visual search. *Journal of Cognitive Neuroscience*, *21*, 760–775. https://doi.org/10.1162/jocn.2009.21039, PubMed: 18564048

Koivisto, M., & Silvanto, J. (2012). Visual feature binding: The critical time windows of V1/V2 and parietal activity. *Neuroimage*, *59*, 1608–1614. https://doi.org/10.1016/j.neuroimage.2011.08.089, PubMed: 21925610

Lamme, V. A., & Roelfsema, P. R. (2000). The distinct modes of vision offered by feedforward and recurrent processing. *Trends in Neurosciences*, *23*, 571–579. https://doi.org/10.1016/S0166-2236(00)01657-X, PubMed: 11074267

Luck, S. J., Girelli, M., McDermott, M. T., & Ford, M. A. (1997). Bridging the gap between monkey neurophysiology and human perception: An ambiguity resolution theory of visual selective attention. *Cognitive Psychology*, *33*, 64–87. https://doi.org/10.1006/cogp.1997.0660, PubMed: 9212722

Luck, S. J., & Hillyard, S. A. (1994). Electrophysiological correlates of feature analysis during visual search. *Psychophysiology*, *31*, 291–308. https://doi.org/10.1111/j.1469-8986.1994.tb02218.x, PubMed: 8008793

Luria, R., & Vogel, E. K. (2011). Shape and color conjunction stimuli are represented as bound objects in visual working memory. *Neuropsychologia*, *49*, 1632–1639. https://doi.org/10.1016/j.neuropsychologia.2010.11.031, PubMed: 21145333

Maier, M., Steinhauser, M., & Hübner, R. (2008). Is the error-related negativity amplitude related to error detectability? Evidence from effects of different error types. *Journal of Cognitive Neuroscience*, *20*, 2263–2273. https://doi.org/10.1162/jocn.2008.20159, PubMed: 18457501

Mathewson, K. E., Beck, D. M., Ro, T., Maclin, E. L., Low, K. A., Fabiani, M., et al. (2014). Dynamics of alpha control: Preparatory suppression of posterior alpha oscillations by frontal modulators revealed with combined EEG and event-related optical signal. *Journal of Cognitive Neuroscience*, *26*, 2400–2415. https://doi.org/10.1162/jocn_a_00637, PubMed: 24702458

Mathewson, K. E., Gratton, G., Fabiani, M., Beck, D. M., & Ro, T. (2009). To see or not to see: Prestimulus α phase predicts visual awareness. *Journal of Neuroscience*, *29*, 2725–2732. https://doi.org/10.1523/JNEUROSCI.3963-08.2009, PubMed: 19261866

Moshagen, M. (2010). multiTree: A computer program for the analysis of multinomial processing tree models. *Behavior*

Research Methods, *42*, 42–54. https://doi.org/10.3758/BRM.42.1.42, PubMed: 20160285

Nieuwenhuis, S., Ridderinkhof, K. R., Blom, J., Band, G. P., & Kok, A. (2001). Error-related brain potentials are differentially related to awareness of response errors: Evidence from an antisaccade task. *Psychophysiology*, *38*, 752–760. https://doi.org/10.1111/1469-8986.3850752, PubMed: 11577898

Prime, D. J., Pluchino, P., Eimer, M., Dell'Acqua, R., & Jolicœur, P. (2011). Object-substitution masking modulates spatial attention deployment and the encoding of information in visual short-term memory: Insights from occipito-parietal ERP components. *Psychophysiology*, *48*, 687–696. https://doi.org/10.1111/j.1469-8986.2010.01133.x, PubMed: 20874751

Prinzmetal, W., Henderson, D., & Ivry, R. (1995). Loosening the constraints on illusory conjunctions: Assessing the roles of exposure duration and attention. *Journal of Experimental Psychology: Human Perception and Performance*, *21*, 1362–1375. https://doi.org/10.1037/0096-1523.21.6.1362, PubMed: 7490585

Prinzmetal, W., Ivry, R. B., Beck, D., & Shimizu, N. (2002). A measurement theory of illusory conjunctions. *Journal of Experimental Psychology: Human Perception and Performance*, *28*, 251–269. PubMed: 11999853

Ro, T. (2019). Alpha oscillations and feedback processing in visual cortex for conscious perception. *Journal of Cognitive Neuroscience*, *31*, 948–960. https://doi.org/10.1162/jocn_a_01397, PubMed: 30912724

Robertson, L. C. (1999). What can spatial deficits teach us about feature binding and spatial maps? *Visual Cognition*, *6*, 409–430. https://doi.org/10.1080/135062899395046

Robitaille, N., & Jolicoeur, P. (2006). Fundamental properties of the N2pc as an index of spatial attention: Effects of masking. *Canadian Journal of Experimental Psychology/Revue Canadienne de Psychologie Expérimentale*, *60*, 101–111. https://doi.org/10.1037/cjep2006011, PubMed: 17133886

Roelfsema, P. R. (2023). Solving the binding problem: Assemblies form when neurons enhance their firing rate—They don't need to oscillate or synchronize. *Neuron*, *111*, 1003–1019. https://doi.org/10.1016/j.neuron.2023.03.016, PubMed: 37023707

Sawaki, R., Geng, J. J., & Luck, S. J. (2012). A common neural mechanism for preventing and terminating the allocation of attention. *Journal of Neuroscience*, *32*, 10725–10736. https://doi.org/10.1523/JNEUROSCI.1864-12.2012, PubMed: 22855820

Singer, W., & Gray, C. M. (1995). Visual feature integration and the temporal correlation hypothesis. *Annual Review of Neuroscience*, *18*, 555–586. https://doi.org/10.1146/annurev.ne.18.030195.003011, PubMed: 7605074

Tallon-Baudry, C., & Bertrand, O. (1999). Oscillatory gamma activity in humans and its role in object representation. *Trends in Cognitive Sciences*, *3*, 151–162. https://doi.org/10.1016/S1364-6613(99)01299-1, PubMed: 10322469

Treisman, A. (1996). The binding problem. *Current Opinion in Neurobiology*, *6*, 171–178. https://doi.org/10.1016/S0959-4388(96)80070-5, PubMed: 8725958

Treisman, A. M., & Gelade, G. (1980). A feature-integration theory of attention. *Cognitive Psychology*, *12*, 97–136. https://doi.org/10.1016/0010-0285(80)90005-5, PubMed: 7351125

Treisman, A., & Schmidt, H. (1982). Illusory conjunctions in the perception of objects. *Cognitive Psychology*, *14*, 107–141. https://doi.org/10.1016/0010-0285(82)90006-8, PubMed: 7053925

van Kerkoerle, T., Self, M. W., Dagnino, B., Gariel-Mathis, M. A., Poort, J., van der Togt, C., et al. (2014). Alpha and gamma oscillations characterize feedback and feedforward processing in monkey visual cortex. *Proceedings of the National Academy of Sciences, U.S.A.*, *111*, 14332–14341. https://doi.org/10.1073/pnas.1402773111, PubMed: 25205811

Vinck, M., Uran, C., Spyropoulos, G., Onorato, I., Broggini, A. C., Schneider, M., et al. (2023). Principles of large-scale neural interactions. *Neuron*, *111*, 987–1002. https://doi.org/10.1016/j.neuron.2023.03.015, PubMed: 37023720

Vogel, E. K., & Machizawa, M. G. (2004). Neural activity predicts individual differences in visual working memory capacity. *Nature*, *428*, 748–751. https://doi.org/10.1038/nature02447, PubMed: 15085132

Wascher, E., & Beste, C. (2010). Tuning perceptual competition. *Journal of Neurophysiology*, *103*, 1057–1065. https://doi.org/10.1152/jn.00376.2009, PubMed: 20032246

Wessel, J. R., Danielmeier, C., & Ullsperger, M. (2011). Error awareness revisited: Accumulation of multimodal evidence from central and autonomic nervous systems. *Journal of Cognitive Neuroscience*, *23*, 3021–3036. https://doi.org/10.1162/jocn.2011.21635, PubMed: 21268673

Worden, M. S., Foxe, J. J., Wang, N., & Simpson, G. V. (2000). Anticipatory biasing of visuospatial attention indexed by retinotopically specific α-bank electroencephalography increases over occipital cortex. *Journal of Neuroscience*, *20*, RC63. https://doi.org/10.1523/JNEUROSCI.20-06-j0002.2000, PubMed: 10704517

Yuval-Greenberg, S., Tomer, O., Keren, A.S., Nelken, I., & Deouell, L. Y. (2008). Transient induced gamma-band response in EEG as a manifestation of miniature saccades. *Neuron*, *58*, 429–441. https://doi.org/10.1016/j.neuron.2008.03.027, PubMed: 18466752

Zhang, Y., Zhang, Y., Cai, P., Luo, H., & Fang, F. (2019). The causal role of α-oscillations in feature binding. *Proceedings of the National Academy of Sciences, U.S.A.*, *116*, 17023–17028. https://doi.org/10.1073/pnas.1904160116, PubMed: 31383766